Direct Measurement of the Twist Penetration Length in a Single Smectic A Layer of Colloidal Virus Particles†

Edward Barry, Zvonimir Dogic, and Robert B. Meyer*

The Martin Fisher School of Physics, Brandeis University, Waltham, Massachusetts 02454

Robert A. Pelcovits

Department of Physics, Brown University, Providence, Rhode Island 02912

Rudolf Oldenbourg

Marine Biological Laboratory, Woods Hole, Massachusetts 02543, Department of Physics, Brown University, Providence, Rhode Island 02912

Received: July 29, 2008

In the 1970s, deGennes discussed the fundamental geometry of smectic liquid crystals and established an analogy between the smectic A phase and superconductors. It follows that smectic layers expel twist deformations in the same way that superconductors expel magnetic field. We make a direct observation of the penetration of twist at the edge of a single isolated smectic A layer composed of chiral *fd* virus particles subjected to a depletion interaction. Using the LC-PolScope, we make quantitative measurements of the spatial dependence of the birefringence due to molecular tilt near the layer edges. We match data to theory for the molecular tilt penetration profile and determine the twist penetration length for this system.

I. Introduction

In the first edition of *The Physics of Liquid Crystals*, deGennes discusses the fundamental stacked fluid layer geometry of smectic phases, and points out that a unit vector field $\hat{p}$ perpendicular to a continuous layer must have zero twist.[1] Describing the slowly varying deformation of an initially flat layer by a displacement function $u(x, y)$, for small tilts of the layer, $p_x = -\partial u/\partial x$ and $p_y = -\partial u/\partial y$. Then, the twist of the $\hat{p}$ field, $t = (\partial p_y/\partial x - \partial p_x/\partial y) = -(\partial^2 u/\partial y \partial x - \partial^2 u/\partial x \partial y) = 0$.

For the smectic A phase composed of rodlike molecules, the molecules are, on average, perpendicular to the smectic layers. Therefore, over a layer as a whole, the director field $\hat{n}$, which is parallel to the local molecular alignment direction, must have zero twist. However, as discussed in deGennes's seminal paper of 1972, on the analogy between the smectic A phase and a superconductor, by allowing local tilting of $\hat{n}$ relative to the smectic layer normal, one can introduce twist at layer edges or around defects in the smectic phase.[2] This tilt of $\hat{n}$, and the resulting twist, penetrate only a small distance λ_t into the otherwise perfect smectic layer, in analogy with the London penetration length of a magnetic field into a superconductor. In the smectic A phase, experience so far indicates that the twist penetration length is significantly longer than the fundamental ordering coherence length of the smectic phase, so that the smectic A phase is analogous to a type II superconductor.

For a smectic A phase composed of chiral molecules, the tendency to twist is not an externally applied deformation but a natural tendency of the molecular packing that competes with the tendency of the molecules to form smectic layers. If the chiral perturbation on the layer packing is weak, then one has an analogy with a type II superconductor in a magnetic field below its lower critical magnetic field, and twist only penetrates at layer edges, or around isolated defects that may exist in the smectic phase. However, if the tendency to twist is strong enough, it may disrupt the smectic system to the extent of producing a systematic array of screw dislocations throughout the smectic phase, in analogy with penetration of magnetic flux quanta into a type II superconductor above its lower critical magnetic field. This is the physical basis for the formation of the magnificent, widely studied twist grain boundary (TGB) smectic phases.[3−5] In these phases, the molecular tilt relative to the smectic layers is a maximum at each screw dislocation core, and dies away with distance from the core, with a length scale given by λ_t. In this context, the twist penetration length plays a crucial role in the structure and free energy of the TGB phase.

In this paper, we consider a system composed of a finite size monolayer of rodlike virus particles, in which the molecules tend to pack together parallel to the layer normal, so it is effectively like a single layer of a smectic A phase. The molecules are chiral, and have a tendency to form spontaneous twist deformation, which competes with the fundamental layer packing. In the case studied here, the twist tendency is weak enough so that the molecules only tilt, and twist only penetrates, at the edges of the layer, while far from the edges the molecules remain perpendicular to the layer. The unique feature of our system is that the constituent molecules are 880 nm long rodlike viruses. It follows that the resulting characteristic length scale of the system is large enough to be visualized directly with optical microscopy. We make quantitative measurements of the birefringence that is induced by the tilt of the molecules near the layer edge, and compare our experimental results with the theory of twist penetration into the interior of the layer. We find good agreement between theory and experiment and determine the characteristic length of twist penetration for this system.

† Part of the "PGG (Pierre-Gilles de Gennes) Memorial Issue".

10.1021/jp8067377 CCC: $40.75
Published on Web 11/01/2008

II. Theory

For this problem, we simplify the general form of the smectic A free energy presented by deGennes in analogy with superconductors. First, since the smectic layer is flat, and only director tilt occurs, the smectic order parameter is simply a constant. We ignore any change in the order parameter very near the edge of the single smectic layer, in effect ignoring the possible existence of a small but finite coherence length, and focus only on the spatial variation of the director. Here, we consider first a semi-infinite smectic layer in the $x \geq 0$ half-plane, in which the director tilts by angle θ in the y direction, tangential to the edge of the layer. The free energy is then

$$F = \int_0^\infty \left[\frac{1}{2}K_2(\mathrm{d}\theta/\mathrm{d}x - q)^2 + \frac{1}{2}C\sin^2(\theta)\right]\mathrm{d}x \qquad (1)$$

in which the first term is the twist energy density, with K_2 being the twist curvature elastic constant and q the spontaneous twist wave vector. The second term is the tilt energy density. The Euler−Lagrange equation is

$$\lambda_t^2\mathrm{d}^2\theta/\mathrm{d}x^2 - \sin(2\theta) = 0 \qquad (2)$$

in which the twist penetration length is $\lambda_t = (K_2/C)^{1/2}$. This free energy and Euler−Lagrange equation are completely analogous to those for the problem of the remaining twist structure at the edge of a cholesteric sample in a magnetic field large enough to unwind the cholesteric helix. deGennes solved a similar problem for twist at the edge of a nematic sample in a magnetic field.[1] The difference for the cholesteric problem, and for the one we consider here, is the boundary condition that, at $x = 0$, $\mathrm{d}\theta/\mathrm{d}x = q$. The first integral of the Euler−Lagrange equation is $\lambda_t\mathrm{d}\theta/\mathrm{d}x = \pm\sin(\theta)$, and the solution for our case is

$$\theta(x) = 2\arctan[\tan(\theta_0/2)\exp(-x/\lambda_t)] \qquad (3)$$

with $\theta_0 = -\arcsin(q\lambda_t)$. θ_0 is the maximum tilt angle at $x = 0$.

In fact, our samples are disks of various radii, R, so that there are further curvatures in addition to the simple twist of the semi-infinite plane geometry. Again, for tilt of the director tangential to the edge of the disk, and circular symmetry, so that the tilt angle is a function of radius only, the free energy is

$$F = \int_0^R \left[\frac{1}{2}K_2(\hat{n}\cdot\nabla\times\hat{n} - q)^2 + \frac{1}{2}K_3(\hat{n}\times\nabla\times\hat{n})^2 + \frac{1}{2}C\sin^2(\theta)\right]2\pi r\,\mathrm{d}r \qquad (4)$$

$$= \int_0^R \left[\frac{1}{2}K_2\left(\frac{\sin(2\theta)}{2r} + \mathrm{d}\theta/\mathrm{d}r - q\right)^2 + \frac{1}{2}K_3\left(\frac{\sin^4(\theta)}{r^2}\right) + \frac{1}{2}C\sin^2(\theta)\right]2\pi r\,\mathrm{d}r \qquad (5)$$

The K_3 term is the bend energy density. At the center of the disk, $\theta = 0$. We have solved this more complex problem for disks of arbitrary radius using numerical methods and find that, for disks of the size studied here, the solution for the semi-infinite plane sample is almost indistinguishable in shape from the correct solution, except that the maximum tilt at the edge of the disk is significantly different. Therefore, for curve fitting in our data analysis, we were able to use the analytic solution for the semi-infinite plane case, with the maximum tilt angle θ_0 as a fitting parameter. The structure and energetics of small circular disks will be presented elsewhere.

When the smectic layer is viewed from above, in the direction normal to the layer, the interior of the layer is not birefringent. Near the edges, however, the tilt of the director produces a birefringent region. The retardance, R, at a point near the edge with tilt angle θ is proportional to $\sin^2(\theta)$. In addition, R is linearly proportional to the thickness d of the layer, the concentration c of *fd* particles, and the local order parameter S:

$$R = d\Delta n_{sat} cS\sin^2(\theta) \qquad (6)$$

Δn_{sat} is the specific birefringence of a fully aligned bulk sample of *fd* at unit concentration. Δn_{sat} was previously measured to be $(3.8 \pm 0.3) \times 10^{-5}$ mL/mg.[6] The order parameter for *fd* bulk liquid crystalline suspensions at concentrations of approximately 100 mg/mL was measured to be above 0.95. Since the rod concentration within the smectic layer is ~100 mg/mL (see below), to a first-order approximation, it is reasonable to assume that rods within a smectic layer are almost perfectly aligned. Therefore, we set S equal to 1 for our analysis. The change in layer thickness near the edge is not known. If the layer were exactly one rod-length thick, as the rods tilt, their projected length on the layer normal would decrease the layer thickness by a factor of $\cos(\theta)$ and hence decrease the observed retardance. While for small tilt angles the factor $\sin^2(\theta)$ in eq 6 dominates and the expected retardance increases with θ, for tilt angles above 55°, the expected retardance would decrease if the layer thickness would decrease by the factor $\cos(\theta)$. This is inconsistent with our data at the sample edge.

We fitted the retardance data versus distance from the edge to two models, one that includes the factor $\cos(\theta)$ and one that assumes the layer thickness to remain constant right up to the edge of the disk. We find that the derived twist penetration length is independent of the model used, while the maximum tilt angle at the disk edge is model dependent and not as well determined by our analysis.

The image obtained in optical microscopy is characterized by a resolution function, making a perfect point object at location x_0 have a finite width w. w is of the order $\lambda/(2\mathrm{NA})$, with λ being the wavelength of light and NA the numerical aperture of the objective used. The resolution is characterized by an Airy function, which we approximated by the Gaussian $\exp[-(x - x_0)^2/w^2]$. We convolved the theoretical retardance function with the Gaussian to compare our theoretical results with the measured retardance versus distance from the edge of the smectic layer.

III. Experimental Methods

The rodlike viruses used in this report are the 880 nm long filamentous bacteriophage *fd*. The behavior of these particles has been shown to resemble the behavior of hard rods, with one important difference, the formation of a cholesteric instead of a nematic phase.[7,8] With increasing concentration, a pure aqueous suspension of *fd* viruses will form isotropic, cholesteric, and smectic phases. The current hypothesis is that the microscopic origin of the cholesteric phase is a helical superstructure assumed by the semiflexible viruses in aqueous suspension.[9,10] The addition of polymer to suspensions of these rodlike viruses acts to induce attractive depletion interactions among the particles.[11] A wealth of interesting and hierarchical self-assemblage has been shown to exist in such systems.[12,13] One

type of structure formed in such a system is an isolated fluidlike monolayer of rods, or a membrane, resembling a single layer of a smectic A phase. These membranes are exactly the type described by Helfrich[14] for which he drew an analogy between the free energies of lipid bilayers and smectic A liquid crystals. The detailed mechanism for the formation of these colloidal membranes, and their mechanical properties far away from the edges, will be published elsewhere. Here, we use the *fd* monolayers as model isolated smectic A layers, focusing on how the chirality of the constituent molecules affects the phenomenology at the monolayer edges.

fd virus was grown and purified using standard biological procedures.[7] The virus was then mixed with the polymer Dextran (MW 500 000, SigmaAldrich). The final concentrations of rods and polymer in suspension were 17.5 and 47.5 mg/mL, respectively. All samples were prepared in a buffer solution containing 20 mM Tris and 100 mM NaCl, at a pH of 8.0. Membranes initially self-assemble in the bulk suspension but eventually sediment to the coverslip surface due to their high density. In order to suppress nonspecific binding of membranes to the glass surface, the surfaces were coated with a thin layer of agarose. Cleaned coverslips and glass slides where briefly immersed in a hot 0.1% solution of agarose. Even after this treatment, some membranes are pinned at specific points, as evidenced by the absence of fluctuations. These membranes were not used in our analysis.

Phase contrast and fluorescence images were taken on a standard inverted microscope (Nikon TE2000) equipped with a cooled CCD camera (CoolSnap HQ, Roper Scientific). For fluorescence microscopy, individual viruses were labeled with fluorescent dye (Alexa 488, Invitrogen) according to the previously published protocol.[15] Samples were prepared with a precisely known small fraction of fluorescent virus particles, which could be seen individually in the image of a membrane.

To obtain information about the spatial dependence of the orientation of rods within a monolayer, we used a quantitative polarized light microscope (LC-PolScope, Cambridge Research and Instrumentation, Woburn, MA; http://www.cri-inc.com). The LC-PolScope builds on the polarizing microscope by replacing the traditional compensator with a liquid-crystal-based universal compensator.[16] The LC compensator is used to quickly switch the polarization state of the trans-illuminating light. A digital camera captures five raw images of the sample at circular and ellipical polarization settings. The raw images are used to calculate the retardance and slow axis orientation in each pixel of the sample, producing two high resolution images, one of the retardance and one of the slow axis orientation.[17]

We estimated the concentration of *fd* rods in a smectic monolayer by counting the number of fluorescent rods in a finite area disk membrane. We multiplied the number of fluorescent particles with the concentration ratio of unlabeled to labeled particles and divided by the disk area to estimate the number of unlabeled *fd* particles per square micrometer of membrane (3200 particles/μm^2). Thus, the estimated *fd* concentration in a smectic layer is about 100 mg/mL, based on the known molecular weight 1.67×10^7 g/mol.[7] We enter the estimated *fd* concentration into eq 6 together with the previously mentioned quantities for $\Delta n_{sat} = (3.8 \pm 0.3) \times 10^{-5}$ mL/mg and $S = 1$. Assuming a constant membrane thickness of one rod length (~880 nm), the relationship between the observed retardance and the twist angle at a point in the membrane becomes $R = 3.3 \sin^2(\theta)$ nm.

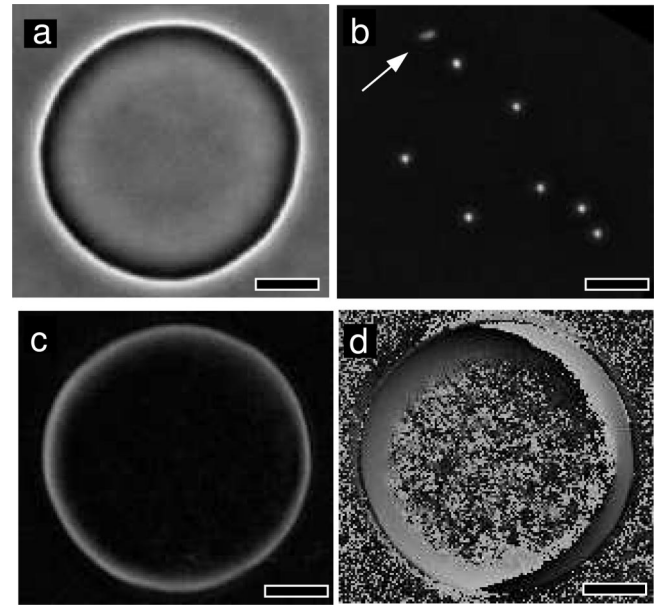

Figure 1. (a) Phase contrast image of a colloidal membrane viewed in a face-on configuration. (b) Image of a membrane in which a small fraction of rods are labeled with a fluorescent dye. Rods near the membrane's edges (indicated by an arrow) appear as short lines, providing direct visual evidence of rod tilting. (c) Retardance image of a membrane. The brightness of each pixel represents the retardance of that point. (d) Orientation image of the slow axis of the birefringence, confirming that rods tilt parallel to the membrane edges. Images in panels c and d were recorded with the LC-PolScope. All scale bars are 5 μm.

IV. Results and Analysis

A phase contrast image of a typical single-layer smectic observed with the monolayer lying in the focal plane of the microscope is shown in Figure 1a. A similar membrane that contains a small fraction of fluorescently labeled rods is examined with a fluorescence microscope (Figure 1b). Far away from the layer's edge, rods are viewed along their axial directions. Consequently, they appear as isotropic dots. Upon closer examination, it becomes evident that rods located within a thin band close to the membrane's edge are tilted with respect to the layer normal. This is a first direct visual evidence of the twist penetration along the membrane's edges. However, fluorescence images are not suitable for quantitative analysis of this effect. To extract quantitative data about the twist penetration length, we examine single monolayers with the LC-PolScope. Far away from the layer edge, all of the rods point perpendicular to the layer surface. Consequently, this region appears isotropic when viewed with the LC-PolScope. At the layer edge, the existence of rod tilting results in a bright birefringent band. The LC-PolScope image shown in Figure 1c confirms the existence of twist penetration. In addition, the map of the slow axis of the birefringence in Figure 1d indicates that rods tilt parallel to the layer edge, in agreement with the fluorescence images.

All image analysis was performed using software written in the IDL programming language. To obtain quantitative data on the spatial decay of birefringence at the monolayer's edge, we first detect the edge using a thresholding and skeletonization procedure. Subsequently, the intensity profiles of LC-PolScope images, $I(x)$, are taken along radial cuts normal to the edge. Individual cuts are by themselves noisy, which prohibits any quantitative analysis. To reduce noise, we average up to a few hundred cuts taken along the edge of a single membrane. For

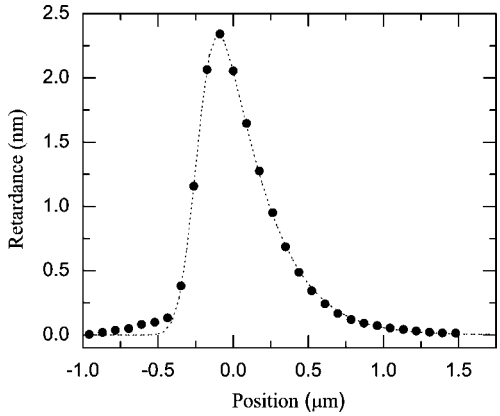

Figure 2. Retardance plotted as a function of the distance from the membrane's edge (+ distance is inside the membrane). The theoretical model (dashed line) is compared to experimental data (full circles). The twist penetration length extracted for this membrane is 0.48 μm.

the averaging procedure to work, we need to translate each cut along the x direction so that all the peaks overlap. Two methods were employed to determine the maximum value of $I(x)$ with subpixel accuracy. Either a derivative is taken, and the signal maximum is determined from where it crosses zero, or the signal is fitted to a Gaussian. Both methods produced equivalent results.

The maximum retardance that would be observed exactly at the layer edge is averaged with neighboring (lower) values by the finite resolution of the microscope, so it is deduced indirectly from the overall curve fitting procedure. Using the edge retardance from the curve fitting procedure to determine the maximum tilt angle at the edge also depends on a precise understanding of how the layer thickness varies near the sample edge. For our analysis, we use the simplest model of constant thickness and an abrupt drop to zero thickness at the sample edge. We have also tried fitting our data with the quantitatively unacceptable model including the $\cos(\theta)$ factor in the theoretical retardance function, and find that the value we extract for the twist penetration length is the same for both models. The maximum tilt angle at the disk edge is model dependent, so it is less well determined by our analysis.

The averaged experimental measurements of the retardance decay function extracted from a typical LC-PolScope image are shown in Figure 2. The agreement between experimental data (filled circles) and the theoretical retardance model convolved with the resolution function (dashed line) is excellent. The width of the peak in retardance at the sample edge, and especially the decay of the measurements outside the edge of the disk (negative x values), are mainly dependent on the width of the resolution function, while the exponential decay of the measurements toward the interior of the disk (positive x values) is dictated by the decay of the molecular tilt function, and is essentially independent of the width of the resolution function. Thus, the determination of the twist penetration length is mostly independent of both the details of the resolution function and the precise behavior of the sample thickness very near the sample edge. For this particular sample, we extract a twist penetration length of $\lambda_t = 0.48 \pm 0.01$ μm. The other parameters determined by the fitting procedure are the maximum tilt angle at a membrane's edge, $\theta_0 = 1.3$ rad, and the resolution width parameter, $w = 0.13$ μm.

It is important to note that the twist penetration length is independent of the intrinsic twist wave vector q of a liquid crystalline material, depending only on the twist elastic constant K_2 and the value of the tilt energy parameter C. The prediction of the theoretical model is that the value of the parameter q only enters into determining the maximum tilt at the disk edge. To verify this experimentally, we need to analyze quantitatively disks of different diameters, since edge curvature affects this boundary value. This analysis will be published elsewhere. In the semi-infinite smectic layer model, the value of q is given by $q = \sin(\theta_0)/\lambda_t$, which results in $q = 2.0$ rad/μm, or a cholesteric pitch of 3.1 μm, a reasonable number for the cholesteric phase of this material.[8] For the curved edge of a finite diameter disk, the relationship between maximum tilt angle and q is not so simple, as will be discussed elsewhere. In general, higher curvature leads to lower values of maximum tilt. This, plus the model dependence of our value for θ_0 means that the value of q derived here is only approximate, while the value of the twist penetration length λ_t is accurately determined.

In conclusion, deGennes long ago presented a clear theoretical understanding of how twist is expelled from layered systems like the smectic A phase, and of how, for a weakly chiral smectic A phase, twist penetrates only at sample edges. We are now able to confirm his insights with direct observations of twist penetration in a single smectic layer, and to measure the important twist penetration length in this system. In the future, we will explore the variation of the twisting strength in our materials, to examine the fascinating regime of strong chirality, in which twist penetrates our two-dimensional single-layer smectic samples as quantized π-twist-wall defects, in analogy with the flux-lattice phase of a type II superconductor, and with the TGB phase of three-dimensional smectics.

Acknowledgment. This work was supported by NSF through grants DMR-0705855 to Z.D. and DMR-0322530 to R.B.M., by NIH grant R01-EB002583 to R.O., and by Brandeis University. R.A.P. wishes to thank the Martin Fisher School of Physics at Brandeis University for their hospitality.

References and Notes

(1) De Gennes, P. G. *The Physics of Liquid Crystals*; Clarendon Press: Oxford U.K., 1974.
(2) DeGennes, P. G. *Solid State Commun.* **1972**, *10*, 753.
(3) Renn, S. R.; Lubensky, T. C. *Phys. Rev. A* **1988**, *38*, 2132.
(4) Goodby, J. W.; Waugh, M. A.; Stein, S. M.; Chin, E.; Pindak, R.; Patel, J. S. *Nature* **1989**, *337*, 449.
(5) Fernsler, J.; Hough, L; Shao, R. F.; Maclennan, J. E.; Navailles, L.; Brunet, M.; Madhusudana, N. V.; Mondain-Monval, O.; Boyer, C.; Zasadzinski, J.; Rego, J. A.; Walba, D. M.; Clark, N. A. *Proc. Natl. Acad. Sci.* **2005**, *102*, 14191.
(6) Purdy, K. R.; Dogic, Z.; Fraden, S.; Rühm, A.; Lurio, L.; Mochrie, S. G. J. *Phys. Rev. E* **2003**, *67*, 031708.
(7) Dogic, Z.; Fraden, S. *Curr. Opin. Colloid Interface Sci.* **2006**, *11*, 47.
(8) Dogic, Z.; Fraden, S. *Langmuir* **2000**, *16*, 7820.
(9) Grelet, E.; Fraden, S. *Phys. Rev. Lett.* **2003**, *90*, 198302.
(10) Tomar, S.; Green, M. M.; Day, L. A. *J. Am. Chem. Soc.* **2007**, *129*, 3367.
(11) Asakura, S.; Oosawa, F. *J. Chem. Phys.* **1954**, *22*, 1255.
(12) Alsayed, A. M.; Dogic, Z.; Yodh, A. G. *Phys. Rev. Lett.* **2004**, *93*, 057801.
(13) Dogic, Z. *Phys. Rev. Lett.* **2003**, *91*, 165701.
(14) Helfrich, W. *Z. Naturforsch.* **1973**, *28*, 693.
(15) Lettinga, M. P.; Barry, E.; Dogic, Z. *Europhys. Lett.* **2005**, *71*, 692.
(16) Oldenbourg, R.; Mei, G. *J. Microsc.* **1995**, *180*, 140.
(17) Shribak, M.; Oldenbourg, R. *Appl. Opt.* **2003**, *42*, 3009.

JP8067377